ASTRONOMY & ASTROPHYSICS
SUPPLEMENT SERIES

Astron. Astrophys. Suppl. Ser. **128,** 581-588 (1998)

Effective collision strengths for electron impact excitation of Xe III, Xe IV, Xe VI and Ba II, Ba IV

T. Schöning and K. Butler

Institut für Astronomie und Astrophysik der Universität München, Scheinerstr. 1, D-81679 München, Germany

Received February 12; accepted July 24, 1997

Abstract. Effective electron excitation collision strengths have been calculated for fine-structure forbidden transitions within the $5p^k$ ($k = 1, 3, 4$) ground configurations of Xe III, Xe IV, Xe VI and the $5p^5$ configuration of Ba IV. In addition calculations have been performed for allowed and forbidden transitions within the three lowest configurations of Ba II. For astrophysical applications the data are tabulated in the range $2\,000 - 50\,000$ K. The applicability of the Breit-Pauli R-matrix technique to the computation of collision strengths for xenon and barium ions has been investigated by comparison with test calculations using the Dirac R-matrix method. Our data will be employed in quantitative analyses of highly excited nebular spectra, especially of NGC 7027 where important implications for the interpretation of collisionally excited transitions in the heavy ions are expected.

Key words: atomic data — plasmas — planetary nebulae: NGC 7027

1. Introduction

Calculations of collisional data for heavy trace elements have been stimulated by the recent detection of collisionally excited lines of krypton, xenon and barium ions in the spectrum of the planetary nebula (PN) NGC 7027 (Péquignot & Baluteau 1994, hereafter referred to as PB94). In a previous paper (Schöning 1996, hereafter Paper I) we have presented effective collision strengths for transitions within the $4p^k$ ($k = 2-4$) ground configuration of Kr III, IV, V. The calculations have important implications for analyses of the nebular krypton lines. We have shown that the collision strengths for krypton ions are similar in magnitude to those for homologous transitions in lighter noble gas ions and thus cannot account for the anomalous intensities of the collisionally excited krypton lines in NGC 7027.

Unexpectedly large line intensities have also been measured for the xenon and barium ions identified in NGC 7027. Péquignot & Baluteau have discussed the plausible explanation that the abundances of the heavy elements in the PN are enhanced by roughly an order of magnitude relative to the solar system values. The authors suggest that the process of nucleosynthesis in low-mass stars and the subsequent injection of its by-products into the interstellar medium be carefully reinvestigated using reliable elemental abundances. Thus detailed quantitative analyses of the Xe III, IV, VI and Ba II,IV lines are needed which make it necessary to have accurate electron collision strengths available.

We have performed preliminary calculations of effective collision strengths for Xe IV (Schöning 1995) using the non-relativistic R-matrix theory (Berrington et al. 1987). In this work fine-structure splitting of the target terms has been approximately included through algebraic transformations of the LS-coupling transmission matrices to intermediate coupling. Since the applicability of the non-relativistic method is restricted to low-Z ions the resulting collision strengths are considered to be only rough estimates. Nevertheless, the data proved to be useful for examining the gross behaviour of the effective collision strengths of heavy noble gas ions.

For heavy ions such as xenon ($Z = 54$) and barium ($Z = 56$) relativistic effects are important. For instance the target structure and, consequently, the target thresholds in the collision strengths as a function of colliding electron energy are significantly affected by fine-structure splitting. Thus, within the framework of the close-coupling approach, these effects have to be consistently included in the target and scattered electron wavefunction from the outset. With regard to the relatively high nuclear charge of the complex ions the Dirac R-matrix theory (see Norrington & Grant 1987) is the state of art for solving the electron scattering problem in a $J - J$ coupling representation. However, since these calculations are extremely demanding in terms of computing time it is impractical to produce large amounts of collisional data with the presently available computing facilities. Hence, as in Paper I we have tackled the electron scattering problem using the low-Z Breit-Pauli

formulation of the R-matrix method (Hummer et al. 1993: The IRON Project, hereafter IP93). Here the non-relativistic continuum Hamiltonian is transformed from LS-coupling to a pair coupling scheme and the one-body mass correction, Darwin and spin-orbit terms are additionally included. It is well known that the Breit-Pauli Hamiltonian is applicable to intermediate Z-ions with Z not much beyond $Z = 30$. We expect, however, that with increasing electron temperature (i.e. higher collisional energies) relativistic target effects will play a minor rôle in the scattering process. Thus for selected ions we have compared the Breit-Pauli collision strengths with test calculations using the Dirac R-matrix method in order to estimate the accuracy of our results and to clarify the question as to whether our data can be used to provide reliable diagnostics for highly excited nebular spectra. Furthermore, analogously to the case of krypton ions, we have investigated the applicability of the semi-relativistic R-matrix method, an extension of the non-relativistic R-matrix theory, as an adequate alternative to the costly Breit-Pauli calculations.

In the following section (Sect. 2) we will briefly outline the various approaches for the calculation of effective collision strengths for the ions of xenon and barium under consideration: semi-relativistic (TCC), Breit-Pauli (BP) and Dirac (DC) R-matrix methods. Subsequently the BP results are presented in Sect. 3. For selected transitions a comparison of the different methods is critically discussed (Sect. 4). Finally, concluding remarks are given in Sect. 5.

2. Calculations

In the following sections we only sketch the atomic structure and scattering calculations since detailed descriptions of the various methods are to be found elsewhere (IP93, Norrington & Grant 1987).

2.1. Semi-relativistic and Breit-Pauli R-matrix method

To begin with we recall that a consistent treatment of relativistic effects in both the target and scattered electron wavefunction such as in the BP method tends to lead to a problem of prohibitively large dimensions. This is due to the number of scattering channels in the R-matrix which are associated with the target fine-structure levels. They increase rapidly with the number of target terms included. Thus we employ close-coupling representations for the total wavefunctions target + electron based on a reasonably small number of target terms. We have generated configuration-interaction target wavefunction expansions using 7 (Xe III), 10 (Xe IV), 6 (Xe VI), 5 (Ba II) and 3 (Ba IV) LS terms. A compilation of the spectroscopic and correlation target configurations is to be found in Table 1. The one-electron orbitals nl have been optimized using the SUPERSTRUCTURE package (Eissner et al. 1974; Nussbaumer & Storey 1978). Table 2 shows the corresponding adjustable scaling parameters λ_{nl} in the statistical-model potential. From Table 3 it is obvious that the agreement between the calculated fine-structure energy levels and the experimental measurements generally is better than 10%. Nevertheless in the scattering calculations we have adjusted the theoretical target threshold energies to those measured except for a few levels where experimental energies are not available. We note that in Table 3 we have reordered the designation of some calculated levels, e.g. $^2S_{1/2}$ and $^2P_{1/2}$ in Xe VI. These levels

Table 1. Configurations included in the target representations. All configurations include $1s^2 2s^2 2p^6 3s^2 3p^6 3d^{10} 4s^2 4p^6 4d^{10}$

Xe III	Xe IV	Xe VI	Ba II	Ba IV
$4f5s^2 5p^3$	$4f5s^2 5p^2$	$4f^2 5s$	$5s^2 5p^6 5d$	$4f5s^2 5p^4$
$5s^2 5p^4$	$5s^2 5p^3$	$4f5s^2$	$5s^2 5p^6 6s$	$4f5s5p^5$
$5s^2 5p^3 5d$	$5s^2 5p^2 5d$	$4f5s5p$	$5s^2 5p^6 6p$	$5s^2 5p^5$
$5s^2 5p^3 5f$	$5s^2 5p5d^2$	$4f5p5d$	$5s^2 5p^6 6d$	$5s^2 5p^4 5d$
$5s^2 5p^3 6s$	$5s5p^4$	$5s^2 5p$	$5s^2 5p^6 7s$	$5s^2 5p^4 6d$
$5s^2 5p^2 5d^2$	$5s5p^3 5d$	$5s^2 5d$	$5s^2 5p^5 5d6p$	$5s^2 5p^4 7d$
$5s^2 5p5d^3$	$5s5p^2 5d^2$	$5s^2 5f$	$5s^2 5p^5 6s6p$	$5s5p^6$
$5s5p^5$	$5p^5$	$5s5p^2$	$5s^2 5p^5 6p^2$	$5s5p^5 5d$
$5s5p^4 5d$	$5p^4 5d$	$5s5p5d$	$5s^2 5p^5 6p6d$	
$5s5p^3 5d^2$	$5p^3 5d^2$	$5s5p5f$	$5s^2 5p^5 6p7s$	
$5p^6$		$5s5d^2$		
$5p^5 5d$		$5p^3$		
$5p^4 5d^2$		$5p^2 5d$		
		$5p5d^2$		

Table 2. Values for the adjustable scaling parameters λ_{nl} in the statistical-model potential used to calculate the one-electron orbitals

	Xe III	Xe IV	Xe VI	Ba II	Ba IV
λ_{1s}	1.4065	1.4067	1.4066	1.4053	1.4048
λ_{2s}	1.1252	1.1250	1.1249	1.1240	1.1236
λ_{2p}	1.0776	1.0774	1.0769	1.0769	1.0764
λ_{3s}	1.0559	1.0556	1.0553	1.0571	1.0567
λ_{3p}	1.0393	1.0391	1.0386	1.0404	1.0399
λ_{3d}	1.0242	1.0239	1.0235	1.0252	1.0248
λ_{4s}	1.0499	1.0494	1.0478	1.0564	1.0558
λ_{4p}	1.0461	1.0461	1.0449	1.0518	1.0515
λ_{4d}	1.0467	1.0470	1.0453	1.0533	1.0530
λ_{4f}	1.0610	1.0634	0.9918		1.0474
λ_{5s}	1.0594	1.0606	1.0560	1.0707	1.0752
λ_{5p}	1.0676	1.0664	1.0566	1.0728	1.0811
λ_{5d}	1.1116	1.0980	1.0707	1.0871	1.0612
λ_{5f}	1.0853		1.0134		
λ_{6s}	1.2491			1.0837	
λ_{6p}				1.1268	
λ_{6d}				1.0910	1.1573
λ_{7s}				1.0861	
λ_{7d}					1.2776

Table 3. Xe III, IV, VI and Ba II, IV fine-structure energy levels in Ryd. Columns BP contain the calculated SUPERSTRUCTURE results. The experimental values are also given

Xe III	Obs.[a]	BP	Xe IV	Obs.[b]	BP	Xe VI	Obs.[c]	BP
$5s^25p^4\ ^3P_2$	0.0	0.0	$5s^25p^3\ ^4S^o_{3/2}$	0.0	0.0	$5s^25p\ ^2P^o_{1/2}$	0.0	0.0
$^3P_1$	0.08925	0.09002	$^2D^o_{3/2}$	0.12090	0.13221	$^2P^o_{3/2}$	0.14215	0.13104
$^3P_0$	0.07409	0.07829	$^2D^o_{5/2}$	0.15957	0.17024	$5s5p^2\ ^4P_{1/2}$	—	0.78493
$^1D_2$	0.15582	0.16465	$^2P^o_{1/2}$	0.25549	0.27424	$^4P_{3/2}$	—	0.84614
$^1S_0$	0.32900	0.34103	$^2P^o_{3/2}$	0.32486	0.33678	$^4P_{5/2}$	—	0.90621
$5s5p^5\ ^3P^o_2$	0.89544	0.89138	$5s5p^4\ ^4P_{1/2}$	0.99560	0.97653	$^2D_{3/2}$	1.13790	1.10225
$^3P^o_1$	0.94379	0.94508	$^4P_{3/2}$	0.97436	0.95373	$^2D_{5/2}$	1.17763	1.12862
$^3P^o_0$	0.98721	0.98809	$^4P_{5/2}$	0.90820	0.88848	$^2P_{1/2}$	1.29252	1.32147
$^1P^o_1$	1.08465	1.13247	$^2D_{3/2}$	1.11109	1.13357	$^2P_{3/2}$	1.44994	1.49561
$5s^25p^35d\ ^5D^o_4$	1.02310	1.08250	$^2D_{5/2}$	1.14341	1.15894	$^2S_{1/2}$	1.43977	1.45668
$^5D^o_3$	1.01703	1.07244	$^1S_{1/2}$	1.37362	1.41206	$5s^25d\ ^2D_{3/2}$	1.64256	1.68784
$^5D^o_2$	1.01931	1.07194	$5s^25p^25d\ ^2P_{1/2}$	1.24657	1.29287	$^2D_{5/2}$	1.66132	1.70721
$^5D^o_1$	1.02472	1.07405	$^2P_{3/2}$	1.21223	1.25997			
$^5D^o_0$	1.02695	1.07325	$^4F_{3/2}$	1.23003	1.28973			
$^3D^o_3$	1.10473	1.17872	$^4F_{5/2}$	1.24384	1.31168			
$^3D^o_2$	1.06837	1.14450	$^4F_{7/2}$	1.29061	1.35729			
$^3D^o_1$	1.11105	1.18585	$^4F_{9/2}$	1.33062	1.41806			
			$^2F_{5/2}$	1.29240	1.36066			
			$^2F_{7/2}$	1.32143	1.39262			
			$^4D_{1/2}$	1.32232	1.37085			
			$^4D_{3/2}$	1.33232	1.38798			
			$^4D_{5/2}$	1.35491	1.41955			
			$^4D_{7/2}$	1.42032	1.49284			

Ba II	Obs.[d]	BP	Ba IV	Obs.[e]	BP
$5s^25p^66s\ ^2S_{1/2}$	0.0	0.0	$5s^25p^5\ ^2P^o_{3/2}$	0.0	0.0
$5s^25p^65d\ ^2D_{3/2}$	0.04441	0.04779	$^2P^o_{1/2}$	0.15992	0.16672
$^2D_{5/2}$	0.05171	0.05856	$5s5p^6\ ^2S_{1/2}$	1.14643	1.14358
$5s^25p^66p\ ^2P^o_{1/2}$	0.18464	0.19546	$5s^25p^45d\ ^4D_{7/2}$	—	1.36803
$^2P^o_{3/2}$	0.20005	0.21806	$^4D_{5/2}$	1.31188	1.35983
$5s^25p^67s\ ^2S_{1/2}$	0.38597	0.38870	$^4D_{3/2}$	1.31757	1.36843
$5s^25p^66d\ ^2D_{3/2}$	0.41872	0.41758	$^4D_{1/2}$	1.33520	1.39080
$^2D_{5/2}$	0.42060	0.42032			

[a] Persson et al. (1988)
[b] Tauheed et al. (1993)
[c] Kaufman & Sugar (1987)
[d] Moore C.E. (1958)
[e] Sansonetti et al. (1993).

are strongly mixed by spin-orbit coupling and it is well known that SUPERSTRUCTURE could yield incorrect term designations. However, this does not imply that the wavefunctions of these target states are inaccurate.

As in Paper I we apply the following approaches to the solution of the electron scattering problem with the inclusion of relativistic effects: (a) the semi-relativistic TCC and (b) the full intermediate coupling BP R-matrix method for the large-scale calculations. In the TCC method the collisional problem is efficiently solved in LS-coupling and collision strengths for transitions between fine-structure target levels are obtained through algebraic recoupling of the transmission matrices ($T = 1 - S$) to intermediate coupling. Additionally $J - J$ coupling between the target terms is included using a perturbation treatment with term-coupling coefficients (Saraph 1978). Clearly the applicability of this approach must be carefully investigated since it requires the term splittings to be small compared to the term separations. On the other hand the BP Hamiltonian contains the spin-orbit interaction and algebraic recoupling of the Hamiltonian matrices from LS

to a pair coupling scheme includes all scattering channels explicitly including fine-structure.

The numerical solution of the scattering problem is achieved by means of the RAL version of the Iron Project R-matrix package (Eissner, priv. commun.) which can be run both in (a) LS and (b) intermediate coupling mode. Subsequently we employ the asymptotic region codes STGFJ (IP93) and STGFJJ (Eissner, priv. commun.) to calculate the collision strengths for case (a) and (b) respectively. For simplicity channel coupling has been neglected and Coulomb wavefunctions have been used in the asymptotic region. Test calculations have revealed that this approximation affects the collision strengths by $\sim 30\%$ at most for ions with residual charge $z = 1$ but the effect of channel coupling decreases rapidly with increasing z.

Partial wave contributions are included for all total angular momenta and parity symmetries with $J \leq \frac{31}{2}$ for Xe III, $J \leq \frac{32}{2}$ for Xe IV and Xe VI, $J \leq \frac{40}{2}$ for Ba IV and $J \leq \frac{50}{2}$ for Ba II. With this choice, convergence for all the collision strengths could be achieved except for the dipole allowed transitions in Ba II where a new "top-up" procedure in STGFJJ was employed to estimate the contribution of high partial waves. The energy mesh was determined in terms of the effective quantum number ν relative to the next higher target threshold. Particularly narrow resonance structures of the collision strengths could be resolved with a small step width $\Delta\nu = 1\ 10^{-4}$. However, close to thresholds where ν exceeds a value of $\nu_{\max} = 10$ we have used a constant interval length $\Delta E \approx 1\ 10^{-5}$ Ryd in (z-scaled) energy and the resonances have been averaged according to Gailitis' method (Gailitis 1963).

2.2. Dirac R-matrix method

Since we have applied the BP approach to the computation of collision strengths for heavy ions of xenon and barium it is desirable to estimate the accuracy of our results by comparison with the DC method. We consider Xe IV as a test case and employ the multiconfiguration Dirac-Fock code GRASP[2] of Parpia et al. (1996) to obtain wavefunctions and energies for the 10 lowest jj-coupled configuration-state functions (CSF) formed from $5s^25p^3$ and $5s5p^4$ (Table 4). Apart from $4f5s^25p^2$ and $5s5p^25d^2$ all correlation configurations from Table 1 have been included so that the computational dimensions could be kept to a reasonably small level. The self-consistent orbital calculation was performed in the extended average level (EAL) mode which involves an optimisation of the Hamiltonian trace weighted by the degeneracies of the particular CSF. We note that in our calculation only the Coulomb electron-electron interaction is included in the Hamiltonian and higher-order terms such as full transverse Breit and quantum electrodynamic contributions have been neglected.

We have applied the DARC package (Norrington, priv. commun.) to the numerical solution of the collisional problem. Because the residual charge of the Xe IV ion is relatively small and the channel energies of less than 10 Ryd are low, the asymptotic equations could be solved using non-relativistic Coulomb wavefunctions. Accordingly collision strengths were obtained from the asymptotic region code DSTGF (Norrington, priv. commun.) which has a structure similar to the BP code STGFJJ. The choice of computational parameters such as the maximum total angular momentum of the partial wave contribution tallies with the corresponding BP calculation.

Table 4. Xe IV fine-structure energy levels (Ryd) used in the Dirac R-matrix method. The results in column DC are from a ten-state multiconfiguration Dirac-Fock EAL calculation. For comparison column BP contains the corresponding SUPERSTRUCTURE results. The experimental values from Tauheed et al. (1993) are also given

Xe IV		Obs.	DC	BP
$5s^25p^3$	$^4S^o_{3/2}$	0.0	0.0	0.0
	$^2D^o_{3/2}$	0.12090	0.15401	0.15164
	$^2D^o_{5/2}$	0.15957	0.19469	0.20206
	$^2P^o_{1/2}$	0.25549	0.29059	0.29641
	$^2P^o_{3/2}$	0.32486	0.35324	0.38215
$5s5p^4$	$^4P_{1/2}$	0.99560	0.99367	1.04365
	$^4P_{3/2}$	0.97436	0.97011	1.01678
	$^4P_{5/2}$	0.90820	0.90842	0.93688
	$^2D_{3/2}$	1.11109	1.14294	1.18177
	$^2D_{5/2}$	1.14341	1.17645	1.22011

3. Results

We have calculated the Maxwellian averaged effective collision strength

$$\Upsilon_{ij} = \int_0^\infty \Omega_{ij}(x) \exp(-x) \mathrm{d}x \tag{1}$$

with $x = E/k_\mathrm{B}T$. Here E is the kinetic energy of the outgoing electron, T the electron temperature in Kelvin and $k_\mathrm{B} = 6.339\ 10^{-6}$ Ryd/K, the Boltzmann constant. The excitation rate coefficient from level i to j is then given by

$$q_{ij} = \frac{8.631\ 10^{-6}}{g_i T^{1/2}} \exp\left(-\frac{E_{ij}}{k_\mathrm{B}T}\right) \Upsilon_{ij}\ \ \mathrm{cm^3 s^{-1}} \tag{2}$$

where g_i is the statistical weight of level i and E_{ij} the excitation energy of level j relative to i in Ryd. Finally, the de-excitation rate coefficient obeys the relation

$$q_{ji} = \frac{8.631\ 10^{-6}}{g_j T^{1/2}} \Upsilon_{ij}\ \ \mathrm{cm^3 s^{-1}}. \tag{3}$$

We have tabulated Υ_{ij} for all transitions within the ground configurations of Xe III,IV,VI and Ba IV in Table 5.

Table 5. Effective collision strengths for Xe III, IV, VI and Ba II, IV. The left-hand column indicates the values of the electron temperature (Kelvin). In the row containing the ion symbol the indices of the initial and final levels are coded as follows:

Xe III 1. $^3P_2$ 2. $^3P_0$ 3. $^3P_1$ 4. $^1D_2$ 5. $^1S_0$
Xe IV 1. $^4S^\circ_{3/2}$ 2. $^2D^\circ_{3/2}$ 3. $^2D^\circ_{5/2}$ 4. $^2P^\circ_{1/2}$ 5. $^2P^\circ_{3/2}$
Xe VI 1. $^2P^\circ_{1/2}$ 2. $^2P^\circ_{3/2}$
Ba II 1. $^2S_{1/2}$ 2. $^2D_{3/2}$ 3. $^2D_{5/2}$ 4. $^2P^\circ_{1/2}$ 5. $^2P^\circ_{3/2}$
Ba IV 1. $^2P^\circ_{3/2}$ 2. $^2P^\circ_{1/2}$

Xe III	1–2	1–3	1–4	1–5	2–3	2–4	2–5	3–4	3–5	4–5
2 000	3.965	10.610	12.276	0.659	2.454	2.936	1.298	5.079	1.301	2.991
4 000	4.011	10.461	12.014	0.704	2.403	2.788	1.438	5.156	1.410	2.838
6 000	3.927	10.159	11.738	0.792	2.330	2.641	1.475	5.202	1.484	2.801
8 000	3.799	9.830	11.440	0.875	2.264	2.515	1.468	5.212	1.517	2.801
10 000	3.663	9.505	11.139	0.939	2.210	2.410	1.442	5.194	1.524	2.810
12 000	3.531	9.199	10.847	0.984	2.165	2.322	1.406	5.156	1.515	2.819
14 000	3.409	8.916	10.569	1.014	2.127	2.244	1.364	5.105	1.496	2.824
16 000	3.297	8.657	10.305	1.034	2.092	2.176	1.322	5.046	1.472	2.827
18 000	3.195	8.419	10.056	1.045	2.060	2.115	1.279	4.982	1.444	2.827
20 000	3.102	8.202	9.821	1.050	2.029	2.059	1.238	4.915	1.415	2.824
50 000	2.313	6.291	7.515	0.940	1.669	1.565	0.839	4.052	1.073	2.710

Xe IV	1–2	1–3	1–4	1–5	2–3	2–4	2–5	3–4	3–5	4–5
2 000	3.099	2.827	0.630	1.119	5.623	2.468	1.541	2.496	5.108	1.613
4 000	2.922	3.405	0.610	1.301	5.513	2.481	1.831	2.517	5.394	1.677
6 000	2.801	3.533	0.612	1.370	5.391	2.466	1.995	2.517	5.577	1.701
8 000	2.704	3.531	0.628	1.418	5.296	2.453	2.096	2.511	5.703	1.707
10 000	2.626	3.500	0.650	1.463	5.215	2.446	2.168	2.506	5.799	1.707
12 000	2.567	3.468	0.675	1.510	5.145	2.446	2.228	2.504	5.881	1.707
14 000	2.525	3.446	0.703	1.561	5.086	2.452	2.286	2.506	5.960	1.708
16 000	2.497	3.433	0.731	1.616	5.038	2.463	2.344	2.511	6.041	1.713
18 000	2.481	3.430	0.760	1.672	5.002	2.477	2.404	2.520	6.124	1.722
20 000	2.476	3.435	0.789	1.729	4.976	2.494	2.465	2.531	6.210	1.734
50 000	2.727	3.672	1.081	2.226	5.064	2.745	3.121	2.732	7.093	1.966

Xe VI	1–2
2 000	3.680
4 000	3.544
6 000	3.865
8 000	4.307
10 000	4.738
12 000	5.121
14 000	5.449
16 000	5.726
18 000	5.960
20 000	6.157
50 000	7.039

Ba II	1–2	1–3	1–4	1–5	2–3	2–4	2–5	3–4	3–5	4–5
2 000	2.645	4.012	5.916	12.527	8.700	10.969	4.688	4.049	24.553	7.177
4 000	2.724	4.198	6.105	13.380	9.064	11.721	4.991	3.349	26.277	7.171
6 000	2.894	4.459	6.417	14.269	9.274	12.506	5.284	3.053	27.889	7.267
8 000	3.026	4.646	6.765	15.144	9.345	13.236	5.525	2.906	29.304	7.391
10 000	3.107	4.758	7.118	15.983	9.336	13.890	5.717	2.818	30.522	7.504
12 000	3.153	4.819	7.466	16.780	9.288	14.471	5.868	2.755	31.572	7.599
14 000	3.177	4.848	7.807	17.541	9.220	14.992	5.989	2.705	32.490	7.678
16 000	3.187	4.860	8.140	18.272	9.146	15.462	6.087	2.661	33.307	7.747
18 000	3.189	4.861	8.465	18.977	9.069	15.894	6.168	2.621	34.048	7.808
20 000	3.187	4.857	8.784	19.661	8.993	16.295	6.237	2.583	34.730	7.865
50 000	3.162	4.838	13.099	28.569	8.152	20.869	6.853	2.209	42.484	8.599

Ba IV	1–2
2 000	2.622
4 000	2.892
6 000	3.172
8 000	3.468
10 000	3.744
12 000	3.987
14 000	4.196
16 000	4.375
18 000	4.529
20 000	4.663
50 000	5.491

Additionally the results for transitions between states associated with the three lowest configurations of Ba II are listed. The temperature grid with temperatures ranging from 2 000 to 50 000 K has been chosen as to match the conditions in gaseous nebulae and stellar atmospheres.

4. Discussion

In this paper we have applied various R-matrix techniques to the calculation of collision strengths for ions of xenon and barium: the semi-relativistic TCC, the full intermediate coupling BP and the Dirac DC formulation of the R-matrix method. A comparison of the collision strengths as a function of colliding electron energy obtained with the different approaches will demonstrate the influence of appropriately consistent treatments of relativistic effects in the target + electron system on the effective collision strengths. Secondly, deviations between the results of different methods make it possible to estimate the accuracy of our results.

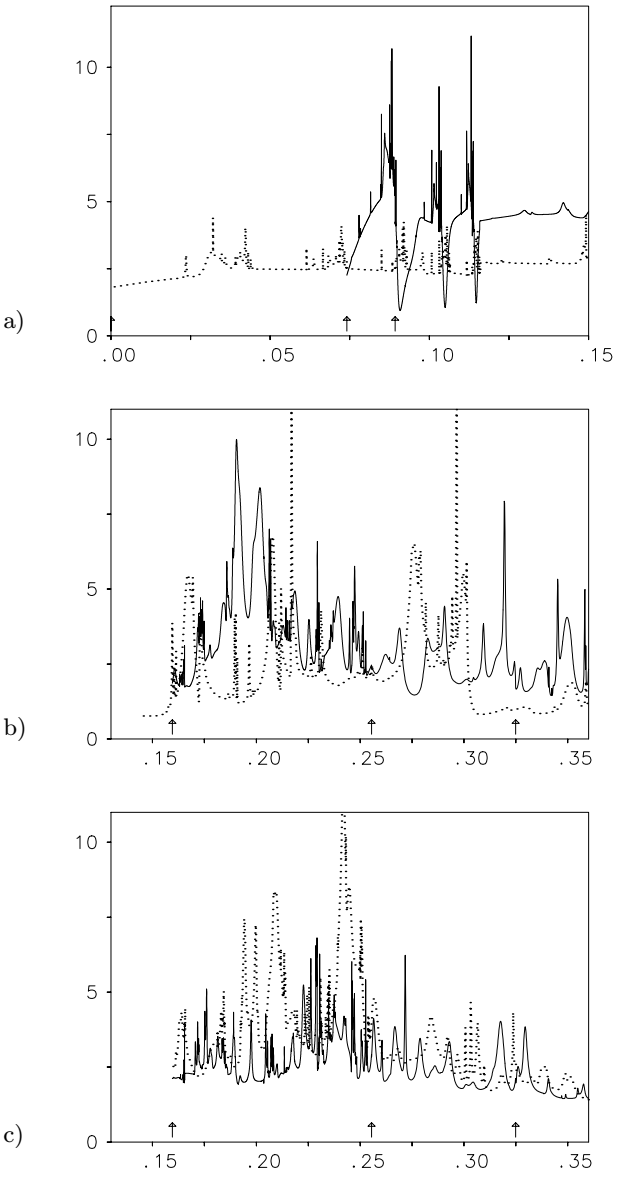

Fig. 1. Collision strength Ω as a function of the incoming electron energy (Ryd) in the near threshold region of the **a)** Xe III $^3P_2 - {}^3P_0$ and **b)** Xe IV $^4S^o_{3/2} - {}^2D^o_{5/2}$ transitions (full curve: BP, dotted: TCC method). **c)** Same as **b)** with the results of our test calculations. Note that here the dotted curve denotes the DC method. The arrows on the energy axis mark the target fine-structure threshold energies

In Paper I we have shown that inclusion of fine-structure splitting in the hamiltonian of krypton ions causes large differences between TCC and BP effective collision strengths especially at low electron temperatures. For xenon ions the level splittings are much larger compared to those of homologous krypton ions and consequently this effect is very prominent in the collision strengths. The fine-structure transition $^3P_2 - {}^3P_0$ in Xe III exhibits a remarkable Rydberg series of resonances close to the excitation threshold which is not at zero energy in the BP calculation (Fig. 1a). This comparison makes clear that for a temperature of 2 000 K BP yields effective collision strengths which exceed the TCC result by a factor of 2 (Fig. 2a). The differences slowly decrease with increasing temperature.

Similarly, the collision strength of the $^4S^o_{3/2} - {}^2D^o_{5/2}$ transition in Xe IV is dominated by complex resonance structures at low energies (Fig. 1b). However, due to the significantly lower background of the TCC calculation the effective collision strengths do not show convergence even at high temperatures (Fig. 2b). This is an indication that the semi-relativistic perturbation approach fails to simulate intermediate coupling effects in the collisional process. Figure 1c illustrates the results of our DC test calculations. It can be seen that at low energies the amplitudes of particular resonances are considerably strengthened whereas the background collision strength is similar to that obtained with the BP method. A maximum deviation of $\sim 30\%$ between the DC and BP effective collision strengths is found at a temperature of 10 000 K (Fig. 2c). Presently this is comparable with other uncertainties in the analyses of highly excited nebular spectra, e.g. due to the determination of ionization equilibria for heavy elements.

Collision strengths have not been measured experimentally for any of the heavy ions. However, in Paper I it has been shown that the effective collision strengths can be inferred from the Θ_λ parameters, determined from the observed line intensities, in Tables 10–13 of PB94. Analogously to Paper I we consider the two transitions in the Xe IV $^4S - {}^2D$ multiplet at 7535.4 Å $(1-2)$ and 5709.2 Å $(1-3)$ where the labelling of the transitions in braces refers to the indices of the fine-structure energy levels in Table 5. Following Eqs. (6), (7) of I we can write

$$\frac{\Theta_{5709}}{\Theta_{7535}} = \frac{\Upsilon_{13}}{\Upsilon_{12}} \tag{4}$$

with Υ_{1j} being the effective collision strength for the transition from the ground state to the upper level j of the line $j \rightarrow i$. The BP calculation using 10 LS terms yields $\Upsilon_{13}/\Upsilon_{12} = 1.4$ for a nebular temperature of 13 500 K (see Table 2 in PB94) which is slightly in disagreement with the measurements ($\Theta_{5709}/\Theta_{7535} = 2.0 \pm 0.4$) of PB94. It is interesting to note that the results of our test calculations with 5 LS terms (BP: $\Upsilon_{13}/\Upsilon_{12} = 1.1$, DC: $\Upsilon_{13}/\Upsilon_{12} = 1.2$) are even further off the observational error limits. This is an indication that better agreement between theory and observation could be achieved with a more detailed target model in the scattering calculations.

Finally, employing our new BP results we plot the effective collision strengths $\Upsilon_{ij}(T = 10\,000\ \mathrm{K})$ for transitions from the ground state to excited states within the np^3 $(n = 2, 3, 4, 5)$ ground configuration of the noble gas ions Ne IV (Giles 1981), Ar IV (Zeippen et al. 1987), Kr IV

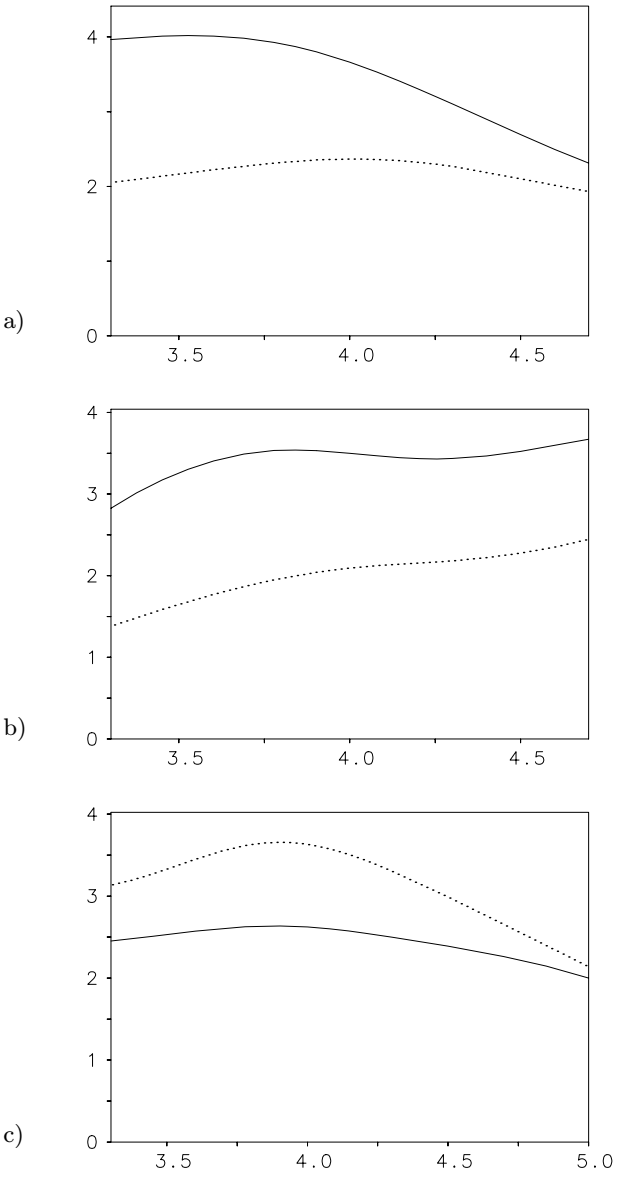

Fig. 2. Effective collision strength Υ as a function of $\log T$(Kelvin) for the transitions **a)** Xe III $^3P_2 - {}^3P_0$ and **b)** Xe IV $^4S^o_{3/2} - {}^2D^o_{5/2}$ (full curve: BP, dotted: TCC method). **c)** Same as **b)** with the results of our test calculations (full curve: BP, dotted: DC method)

(Paper I) and Xe IV (Fig. 3). The diagram exhibits partially monotonic increases of the collision strengths towards higher n. We suspect, however, that the decline of collision strengths for $n > 4$ could be removed with a more elaborate Xe IV target model in a Dirac R-matrix calculation. Nevertheless, a general enhancement of the collision strengths for the heavy noble gas ions by more than an order of magnitude as compared to those of lighter ions which could explain the unexpectedly large intensities of collisionally excited krypton and xenon lines in the spectrum of NGC 7027 can be safely excluded.

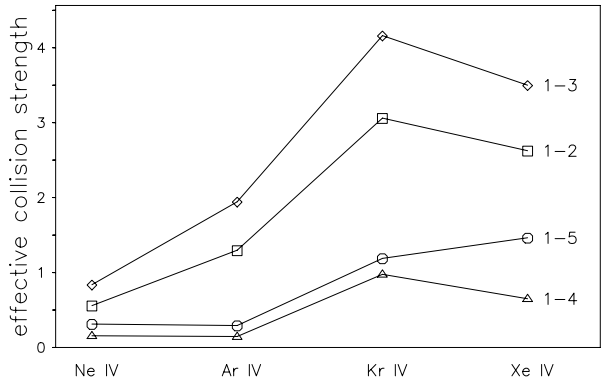

Fig. 3. Effective collision strength $\Upsilon_{ij}(T = 10\,000$ K) for selected homologous transitions in the np^3 ($n = 2, 3, 4, 5$) ground configuration of Ne IV, Ar IV, Kr IV and Xe IV. The transitions are labelled $i - j$ on the right hand side of the diagram with i, j referring to the indices of the fine structure energy levels in Table 5

5. Conclusion

This work is an extension of our previous Breit-Pauli R-matrix calculations of effective collision strengths for krypton ions to elements in the fifth and sixth row of the periodic table. We have shown here that unlike the scattering calculations for krypton ions the semi-relativistic TCC approach, essentially an algebraic recoupling technique using term-coupling coefficients, is not applicable to the computation of collisional data for heavy ions such as Xe III, IV, VI and Ba II, IV. On the other hand, comparison of our BP results with test calculations using the Dirac R-matrix method reveals that the inclusion of relativistic effects in the electron scattering process based on a full intermediate coupling approach yields electron excitation rates of heavy elements which can be used in the derivation of diagnostics for highly excited nebular spectra. The comparison of our results with those for lighter ions confirms our previous conclusions (cf. Paper I) that atomic physics calculations do not corroborate a systematic enhancement of effective collision strengths for heavy elements by orders of magnitude as was suggested in PB94. Consequently the nebular spectrum of NGC 7027 should be carefully reinvestigated using our data to obtain reliable abundances of the heavy ions. With regard to the anomalous intensities of collisionally excited lines new constraints from overabundances of these species are extremely valuable for understanding the process of heavy element formation in the progenitor of NGC 7027 and the subsequent enrichment of the planetary nebula.

Acknowledgements. We thank Drs. W. Eissner, P.H. Norrington and F.A. Parpia for making their program packages available to us. Furthermore TS is indebted to the Deutsche Forschungsgemeinschaft for financial support under grant Bu

703/2-1. The calculations were performed on the Cray Y-MP, T90 computers and the HP cluster of the Bayerische Akademie der Wissenschaften at the Leibniz Rechenzentrum, München. We gratefully acknowledge a grant of computer time by Cray Research Inc. in cooperation with the Leibniz Rechenzentrum.

References

Berrington K.A., Burke P.G., Butler K., et al., 1987, J. Phys. B: At. Mol. Phys. 20, 6379
Eissner W., Jones M., Nussbaumer H., 1974, Comp. Phys. Commun. 8, 270
Gailitis M., 1963, Sov. Phys.-JETP 17, 1328
Giles K., 1981, MNRAS 195, 63P
Hummer D.G., Berrington K.A., Eissner W., et al., 1993, A&A 279, 298 (IP93)
Johnson C.T., Kingston A.E., 1990, J. Phys. B: At. Mol. Opt. Phys., 23, 3393
Kaufman V., Sugar J., 1987, J. Opt. Soc. Am. B 4, 1924
Mendoza C., 1983, Physical Processes in Planetary Nebulae. In: Flower D.R. (ed.) IAU Symp. No. 103, Planetary Nebulae. Reidel, Dordrecht, p. 143
Moore C.E., 1958, Atomic Energy Levels, Vol. III – NBS Circ. 467, Washington, DC
Norrington P.H., Grant I.P., 1987, J. Phys. B: At. Mol. Phys. 20, 4869
Nussbaumer H., Storey P.J., 1978, A&A 64, 139
Parpia F.A., Grant I.P., Fischer C.F., 1996 (in preparation)
Péquignot D., Baluteau J.-P., 1994, A&A 283, 593 (PB94)
Persson W., Wahlström C.-G., Bertuccelli G., et al., 1988, Phys. Scr. 38, 347
Sansonetti C.J., Reader J., Tauheed A., et al., 1993, J. Opt. Soc. Am. B 10, 7
Saraph H.E., 1978, Comp. Phys. Commun. 15, 247
Schöning T., 1995, A&A 299, L25
Schöning T., 1997, A&AS 122, 277 (Paper I)
Sugar J., Musgrove A., 1991, J. Phys. Chem. Ref. Data 20, 859
Tauheed A., Joshi Y.N., Pinnington E.H., 1993, Phys. Scr. 47, 555
Zeippen C.J., Butler K., Le Bourlot J., 1987, A&A 188, 251